

U N I V E R S I T Y O F H A W A I I ' I A T M Ā N O A

Institute for Astronomy

Pan-STARRS Project Management System

The PS4 Telescope Image Budget Allocations

Jeff Morgan
Sr. Telescope Engineer
University of Hawaii
6 March 2008

PSDC-300-027-00

Revision History

Version/Revision	Date	Comments
00	6 Mar 2008	Release of report (still needs retolerancing!)

Table of Contents

1	Scope of Document.....	3
2	Referenced Documents	4
3	Introduction.....	5
4	PS4 Telescope Image Budget Allocations.....	7
4.1	The telescope image budget summary.....	7
4.2	Primary mirror error allocations	9
4.3	Secondary mirror error allocations	12
4.4	L1 corrector error allocations.....	15
4.5	L2 corrector error allocations.....	17
4.6	L3 corrector error allocations.....	18
4.7	Filter error allocations.....	19

List of Figures

Figure 1.	The PS4 baseline optical layout (NOADC-M-2.0.ZMX).	8
Figure 2.	The M1 Polishing Structure Function for the PS4 telescope.	12
Figure 3.	The PS4 Secondary Mirror Structure Function. The red boxes illustrate the data points given in Table 8.....	15

List of Tables

Table 1.	PSDC Documents	4
Table 2.	External Documents.....	4
Table 3.	System Concept Definition Image Budget for PS4	7
Table 4.	Telescope Image Budget.....	9
Table 5.	Primary Mirror Image Budget	10
Table 6.	Primary Mirror Surface Structure Specification.....	10
Table 7.	Secondary Mirror Image Budget	14
Table 8.	Secondary Mirror Structure Function Specification.....	14
Table 9.	L1/ADC Corrector Image Budget.....	16
Table 10.	L2 Corrector Image Budget.....	17

Table 11. L3 Corrector Image Budget 18
Table 12. Filter Image Budget 19

1 Scope of Document

This document reports on the project’s estimates of how the telescope image budget will be allocated amongst collimation errors and manufacturing errors of each of the optical elements in the PS4 telescopes. In large part, this document is nearly a copy of the similar document that was done for the PS1 prototype telescope (PSDC-300-011-02), but it is expected here that deviations will be made when trade-offs between vendor needs and science specifications are done. Note also that these image budgets differ in that the PS1 budget is intended for a Haleakala site while the PS4 budget is intended for a Mauna Kea site.

The telescope image budget is only one part of the whole system image budget, which includes not only the effects of the telescope on the image Point Spread Function (PSF), but also the effects of the camera, the software, and the atmosphere. The system image budget was allocated in PSDC-250-002-00. But because it is necessary for an understanding of many of the numbers used in the tables of this document, the introduction here contains a description for how the image budget for the whole Pan-STARRS system was derived.

2 Referenced Documents

Table 1. PSDC Documents

Pan-STARRS ID	Title	Authors
NOADC-M-2.0.ZMX	The Zemax Optical Layout of the PS4 Telescope Design	Morgan
PSDC-250-002-00	The Pan-STARRS System Concept Definition	The Pan-STARRS Team
PSDC-300-011-02	The PS-1 Telescope Image Budget Allocations	Morgan, Siegmund
PSDC-330-001-02	The System/Subsystem Specification for the Pan-STARRS PS-1 Telescope Subsystem	Morgan, Siegmund
PSDC-330-002-00	The PS-1 Filter Specifications	Siegmund, Morgan, Chambers
PSDC-330-004-00	The Baseline Optical Design for PS-1	Morgan
PSDC-330-005-00	The ADC Drop-in Design for PS-1	Mannery, Morgan

Table 2. External Documents

Source Reference	Title	Authors
http://medusa.as.arizona.edu/lbtwww/tech/ua9401.htm	Optical Design, Error Budget and Specifications for the Columbus Project Telescope	Hill

3 Introduction

The image budget for the Pan-STARRS telescopes flows down from that given in the Pan-STARRS System Concept Definition (the SCD, PSDC-250-002-00). This budget is driven by expectations for the site seeing, charge spreading in the detectors, errors in the image processing algorithms, and by the telescope design.

Table 3 shows the SCD Image Budget as of 26 November 2004. In this table the RMS Radius refers to the Root Mean Square radius of the image Point Spread Function (PSF). The RMS radius of the PSF distribution is related to the normalized Gaussian scale length σ by the equation $\langle r^2 \rangle^{1/2} = \sqrt{2}\sigma$. This characterization of the image budget error is useful when considering the output of ray tracing programs in the design of the optics.

Normally, the Full Width Half Maximum (FWHM) of the PSF is related to σ through the equation $FWHM = 2.354\sigma$, but atmospheric seeing follows Kolmogorov statistics, rather than Gaussian statistics. The best fit Gaussian to a Kolmogorov seeing distribution is found to have $FWHM = 2.0\sigma$. This relation and a telescope plate scale of 38.8 $\mu\text{m}/\text{arcsec}$ (corresponding to a telescope focal length of 8m) is assumed to convert the site seeing of 0.6 arcseconds to an equivalent RMS radius in Table 3. We have

$$\sigma_{\text{seeing}} = \frac{FWHM_{\text{seeing}}}{2.0} \times 38.8 \mu\text{m}/\text{arcsec} = \frac{\langle r^2 \rangle^{1/2}}{\sqrt{2}} = 11.64 \mu\text{m}$$

$$\langle r^2 \rangle^{1/2} = 16.46 \mu\text{m}$$

In the tables below R_0 refers to the Fried parameter which is normally associated with atmospheric seeing. We use the notation of R_0 rather than the more widely used notation of r_0 for the Fried parameter in this documentation in order to avoid confusion between the Fried parameter and the PSF radius, r , which is also used extensively in this document.

For a reference wavelength of 0.5 μm , R_0 is related to the FWHM of the telescope PSF through the equation $FWHM = \frac{10.1}{R_0}$, where R_0 is in centimeters. This relationship is used to convert between columns in Table 3. It is further assumed that the seeing degrades with zenith angle z according to the equation $(R_0)_z = (R_0)_{z=0} \cos^{3/5} z$.

The conversion between R_0 and $\langle r^2 \rangle^{1/2}$ is given by

$$\langle r^2 \rangle^{1/2} = \sqrt{2}\sigma = \frac{\sqrt{2}(FWHM)(38.8 \text{ } \mu\text{m/arcsec})}{2} = \frac{10.1(38.8 \text{ } \mu\text{m/arcsec})}{\sqrt{2}R_0}$$

$$\langle r^2 \rangle^{1/2} = \frac{277.06}{R_0}$$

where R_0 is in cm and $\langle r^2 \rangle^{1/2}$ is in μm .

The R_0 characterization of the image budget is useful when specifying the polish of large optics. This characterization recognizes that the optics in the telescope do not need to be much better than the limitations imposed on the system by the atmosphere itself. A single number characterization of an optical surface, like the RMS surface error, does not account for the fact that at large spatial separations, the atmospheric errors increase.

The R_0 characterization of the errors is effectively a two parameter characterization of the effective surface structure function. The first parameter is a small-scale RMS surface error which effectively characterizes the small angle scattering in the telescope optics and dominates the telescope structure function at small separations (<10 cm). Following Hill's SPIE paper (Optical Design, Error Budget and Specifications for the Columbus Project Telescope, <http://medusa.as.arizona.edu/lbtwww/tech/ua9401.htm>), we assume small angle scattering losses of 5%. For the Pan-STARRS project, the bluest wavelength of observation is 402 nm. Using this as a reference wavelength for the small angle scattering losses gives us the tightest polishing restriction at small spatial separations. However, we are free to do this because mirror polishing typically meets or exceeds fairly tight tolerances at small spatial separations. It is at spatial separations > 10 cm where most of the polishing difficulties are encountered. Using a 5% small angle scattering loss at 402 nm gives us a small scale surface RMS of $\sigma_{ss} = 14.2$ nm. The second parameter is R_0 itself which determines the structure function at large separations and represents a relaxation of the surface errors that would normally be imposed on the system by a simple small-scale RMS surface error.

The Pan-STARRS system PS4 image budget assumes a mean site seeing of $FWHM_{\text{seeing}} = 0.6$ arcseconds. For the Pan-STARRS PS4 detectors it assumes a pixel size of 10 μm . A square pixel with dimension d will convolve with the telescope PSF as a Gaussian with a scale length of $\sigma_{\text{pixel}} = \frac{d}{\sqrt{12}} = 2.89 \text{ } \mu\text{m}$. Charge diffusion in the detector will add to this

profile. Table 3 assumes that charge diffusion in the detector has a Gaussian scale factor of 5.29 μm . This adds in quadrature with the convolution from the finite pixel size of the detector. So, for the camera contributions to the system image budget we have

$$(\sigma_{\text{camera}}^2)^{1/2} = (\sigma_{\text{pixel}}^2 + \sigma_{\text{CD}}^2)^{1/2} = (2.89^2 + 5.29^2)^{1/2} = 36.34^{1/2} = 6.03 \text{ } \mu\text{m}$$

$$\langle r^2 \rangle_{\text{camera}}^{1/2} = \sqrt{2}\sigma_{\text{camera}} = 8.53 \text{ } \mu\text{m}$$

where σ_{CD} is the scale length of charge diffusion in the detector. The IPP contribution is a small contribution to the system PSF from expected errors in the image processing pipeline.

In the System Concept Definition an estimate of the acceptable impacts on the system PSF from the telescope were made based on the science desired out of the Pan-STARRS telescopes. Those estimates are included in Table 3.

Table 3. System Concept Definition Image Budget for PS4

5-Mar-08

PS4 System Image Budget

	RMS Radius (μm)		FWHM (arcsec)		R_0 (cm)	
	$z=0$	$z=70$	$z=0$	$z=70$	$z=0$	$z=70$
Site Seeing	16.46	31.34	0.60	1.14	16.83	8.84
Telescope	9.10	11.50	0.33	0.42	30.45	24.09
Camera	8.53	8.53	0.31	0.31	32.48	32.48
IPP	3.46	3.46	0.13	0.13	80.08	80.08
Total	20.94	34.63	0.76	1.26	93.15	90.14

This report documents how the telescope allocations to the system image budget are distributed to the various telescope subsystems.

4 PS4 Telescope Image Budget Allocations

4.1 The telescope image budget summary

The process of image budget allocation starts with a top-down allocation of the telescope image budget based on the science which is quite independent of any engineering design details. But, in order to break this top level allocation down into component level allocations, it is necessary to have an optical layout in mind.

This document assumes two possible optical layouts for the PS4 telescope. The baseline optical design utilizes 3 refractive elements in the corrector optics. The ADC drop-in design replaces the first corrector element with an Atmospheric Dispersion Corrector (ADC). The remainder of the optics are identical with the baseline layout. The document PSDC-330-004-00 gives the details of the baseline design and the document PSDC-330-005-00 gives details of the ADC design.

Figure 1 shows the optical layout of the PS4 baseline design (NOADC-M-2.0.ZMX). This design is a slight modification to the PS1 baseline design discuss in PSDC-330-004-00. It is in fact identical to the design that was used for the PS1 prototype telescope. The primary and secondary mirrors are designated M1 and M2, respectively. The corrector elements are designated L1, L2, and L3. The last corrector element forms the window of the CCD camera dewar. The design requires the presence of a filter between L2 and L3 for proper focus. The ADC version of the optical layout replaces the thick L1 corrector element with a 3-part,

siloxane filled Atmospheric Dispersion Corrector (ADC) and keeps the physical locations and shapes of the other optics the same. Some of the items in the tables below refer to L1/ADC in recognition of the probable replacement of the first corrector element with the ADC.

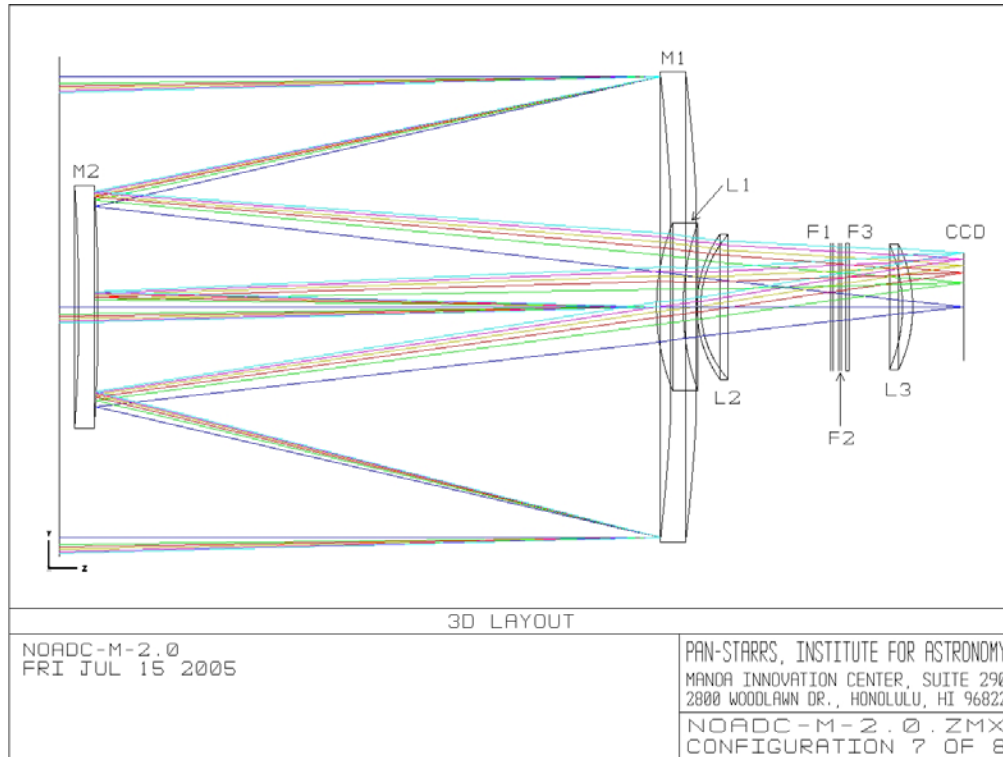


Figure 1. The PS4 baseline optical layout (NOADC-M-2.0.ZMX).

The telescope image budget allocations were made according to the expected contributions to the telescope PSF from the intrinsic design of the telescope and from each optic in the telescope layout. Zemax tolerance calculations were done with the Pan-STARRS ADC design (PSDC-330-005-00) to estimate the impact of each image budget allocation on the physical design of the telescope.

The contributions to the telescope image budget from each optic are shown in Table 4. The summary subtotal in Table 4 was constrained to meet the system image budget telescope allocations shown in Table 3.

Subsequent sections of this document show detailed break-downs of each of the optical elements seen in Table 4. The tables below are our working notes on how the element tolerances of the image budget shown in Table 4 might be distributed. They are an indication to those building the mirror support system of the specifications that will be applied to the polishing of the mirrors. The telescope manufacturers should feel free to redistribute the non-polishing errors as they see fit. Vendors should note that these tables are working notes, subject to change. But the subtotals in these tables are specifications that should be stable.

Table 4. Telescope Image Budget

5-Mar-08

PS4 Telescope Image Budget						
	RMS Radius (um)		R0 (cm)		FWHM (arcsec)	
	z=0	z=70	z=0	z=70	z=0	z=70
Optical Design	6.6	6.6	41.98	41.98	0.24	0.24
M1	3.1	4.4	89.37	62.97	0.11	0.16
M2	1.8	2.3	153.92	120.46	0.07	0.08
L1	2.4	3.3	115.44	83.96	0.09	0.12
L2	2.8	3.5	98.95	79.16	0.10	0.13
L3	1.9	2.2	145.82	125.94	0.07	0.08
Filters	0.5	0.7	554.12	395.80	0.02	0.03
Collimation	2.1	4.4	131.93	62.97	0.08	0.16
Focus	2.0	4.0	138.53	69.27	0.07	0.15
Total	9.07	11.49	30.54	24.11	0.33	0.42
(System Tel. Budget)	9.10	11.50	30.45	24.09	0.33	0.42

4.2 Primary mirror error allocations

Table 5 shows the detailed break-down of errors expected from the primary mirror and its support system. It was assumed here that the primary mirror would be polished on axial supports that very closely resemble the actual mirror support system. It is also assumed that the polishing and testing of the mirror surface can be done to an accuracy that exceeds the telescope surface requirements. Thus, the error allocations for the supports are nearly zero near zenith because the polishing will be done to compensate for the support errors when the telescope is pointed towards the zenith.

The diameter assumed for the primary mirror is shown in the second row of the table. This is a clear aperture diameter, not the actual physical size of the mirror. The units used are millimeters. The last line in Table 5 shows the allocations made for this optic in Table 4.

Zemax tolerance calculations using the macro TEZI were used to verify that if the surface errors were to be randomly distributed, the polishing allocation in Table 5 corresponds to a surface error of ± 59 nm ($\pm 2\text{-}\sigma$ limits of a normal error distribution). This is therefore equivalent to a surface error of $\lambda/10$. The R_0 characterization of the surface errors assumes that the surface errors will not be random, nevertheless, since random surface errors are a common way of describing surface quality, this is a comparison worth mentioning. The polishing allocation is $\frac{1}{2}$ the total error budget.

Figure 2 shows the surface structure function assuming a fine-scale surface roughness of $\sigma_{ss} = 14.3$ nm, an R_0 of 126 cm, and with tilt-compensation. The red squares show the points on the graph given in Table 6. Table 6 is for the convenience of polishing vendors. We describe below the means by which Table 6 and Figure 2 are constructed given values for σ_{ss} and R_0 .

Table 5. Primary Mirror Image Budget

5-Mar-08	PS4 M1 Image Budget					
					D = 1800	
	RMS Radius (um)		R0 (cm)		FWHM (arcsec)	
	z=0	z=70	z=0	z=70	z=0	z=70
Axial Support	0.1	1.0	2770.60	277.06	0.00	0.04
Lateral Support	0.1	2.6	2770.60	106.56	0.00	0.09
Polishing	2.8	2.8	98.95	98.95	0.10	0.10
Actuator Errors	1.0	1.6	277.06	173.16	0.04	0.06
Wind Loading	0.6	1.1	461.77	251.87	0.02	0.04
Glass Inhomogeneity	0.1	0.1	2770.60	2770.60	0.00	0.00
Temp. Non-uniformities	0.1	0.1	2770.60	2770.60	0.00	0.00
Reflective Coating	0.5	0.5	554.12	554.12	0.02	0.02
Subtotal	3.08	4.43	89.94	62.53	0.11	0.16
(Tele. Image Budget)	3.1	4.4	89.37	62.97	0.11	0.16

Table 6. Primary Mirror Surface Structure Specification

Separation (cm)	RMS Surface Error (nm)
1.6	10.8
2.0	11.0
2.5	11.4
3.2	11.9
4.0	12.6
5.0	13.5
6.3	14.6
7.9	16.1
10.0	18.0
12.6	20.4
15.8	23.1
20.0	26.5
25.1	30.3
31.6	34.6
39.8	39.5
50.1	44.7
63.1	49.9

79.4	54.7
100.0	58.1
125.9	57.9
158.5	49.3

The surface structure function specification given in Table 6 is described in detail in the paper “Optical Design, Error Budget and Specifications for the Columbus Project Telescope”, J. Hill, (<http://medusa.as.arizona.edu/lbtwww/tech/ua9401.htm>). The utility of the surface structure function is that it offers a compact way of defining polishing specifications that are matched to the atmospheric limitations imposed on a telescope. This characterization of the polishing recognizes that at low spatial frequencies the polishing specifications may be relaxed because at these frequencies the atmospheric distortions act as a fundamental limit to the wave front.

Hill’s paper gives a justification for the equations used to define the surface structure function. For the calculations here we use Hill’s tilt-compensated equation which accounts for the fact that the tilt terms in the atmospheric distortion may be removed since they do not contribute to PSF degradations and are naturally removed (in part) by telescope pointing. This equation is given by

$$s_{\lambda}(\Delta r) = \left(2\sigma_{ss}^2 + 6.88 \left(\frac{\lambda_{ref}}{2\pi} \right)^2 \left(\frac{\Delta r}{R_0} \right)^{5/3} (\cos z)^{-1} \left(1 - 0.975 \left(\frac{\Delta r}{D} \right)^{1/3} \right) \right)^{1/2}$$

where σ_{ss} is the 1-D RMS small scale surface roughness, λ_{ref} is a reference wavelength, Δr is a spatial separation, R_0 is the atmospheric Fried parameter, and D is the diameter of the optical surface in question. While it can be argued that one should use the diameter of the footprint of the optical beam rather than D in the equation above, doing so results in a precipitous and unmanagable drop in the calculated structure function for surfaces that have radii larger than the footprint diameter. A compromise is to use the diameter of the optical surface itself. For the primary mirror the optical footprint of the beam is identical to the mirror diameter. Therefore, for M1, this is not an issue. But it becomes an important distinction for subsequent optics in the telescope. For subsequent optics, we use the diameter of the optic itself for D rather than the footprint diameter of the optical beam.

The small scale surface roughness, σ_{ss} , is defined by choosing an acceptable level of small angle scattering from the optical surface and then using the equation

$$\% \text{ loss} = \left(\frac{2\pi\sigma_{ss}}{\lambda_{ref}} \right)^2$$

where % loss is the percentage loss of the input beam into small angle scattering. In the calculations for σ_{ss} we have assumed $\lambda_{ref} = 0.402 \mu\text{m}$, and a 5% loss into small angle scattering to derive $\sigma_{ss} = 14.3 \text{ nm}$. For the calculation of $s_{\lambda}(\Delta r)$ we have assumed a more relaxed value of $\lambda_{ref} = 0.61 \mu\text{m}$. In this way we force the small angle scattering to be less

than 5% in all band passes, but limit the surface polishing specifications to be more consistent with the band passes that will be used most commonly in the telescope.

Note that the equation above for $s_\lambda(\Delta r)$ refers to the wave front structure function. The surface structure function for mirrors is given by dividing this equation by 2. In all of the calculations in this document it has been assumed that the testing conditions will be with $z = 0$ degrees. And all of the listed structure functions are surface structure functions.

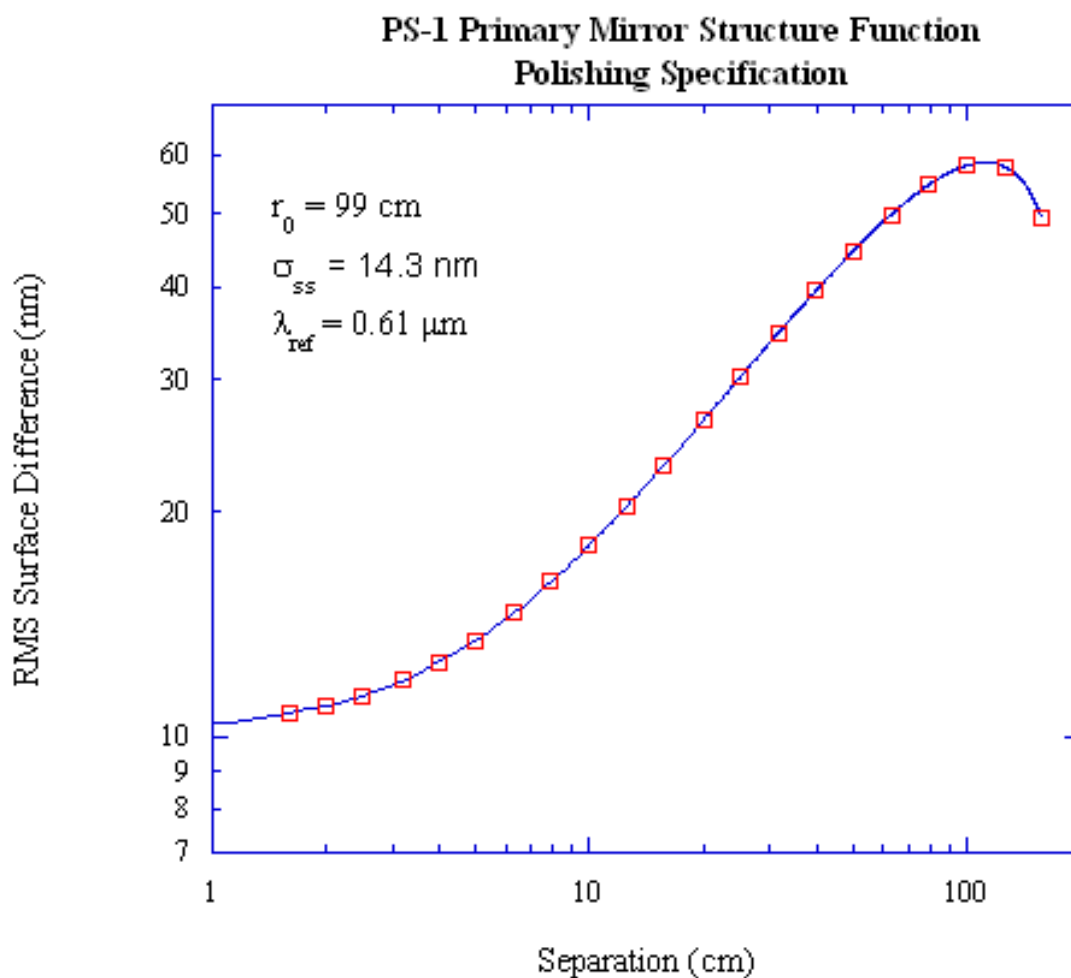


Figure 2. The M1 Polishing Structure Function for the PS4 telescope.

4.3 Secondary mirror error allocations

Optics following the primary mirror are not fully filled by the telescope beam. The secondary diameter for the full telescope field of view of 1.5° is approximately 900 mm in

diameter. However, a point source beam fills only a diameter of 782 mm. This is the footprint diameter that is shown in the table. The ratio between this footprint and the primary mirror clear aperture diameter forms the demagnification factor seen in the first column of the second to last row in Table 7.

Errors listed above the demagnification line in the table are effectively errors that would be seen if the surface errors of the secondary were to be projected back to the surface of the primary mirror. This allows the surface errors to be put in terms of the atmospheric fluctuations characterized by a value of R_0 , but it tends to obscure the true nature of the surface errors on the secondary. For instance in Table 7, an RMS spot radius of $0.1 \mu\text{m}$ does not designate the same size surface errors on the secondary as it does on the primary. Instead, the same spot size in the secondary and primary tables denote actual surface errors that scale roughly as the demagnification ratio, with the surface errors on the secondary being larger. This tends to be a confusion in the following tables.

Like the primary, the secondary error budget is dominated by the polishing errors. In subsequent tables there are budget allocations for alignments of the optics, but no such allocations are made for the secondary. The collimation item in Table 4 is essentially the alignment budget for the secondary mirror. For the purposes of these tables it is assumed that the primary mirror axis is the main fiducial to which all of the other optics are aligned. It therefore needs no allocation for alignment. However, we do not mean to imply here that the primary mirror will not be actively moved during collimation proceedings.

Zemax tolerancing calculations with the macro TEZI were run to confirm that the total image allocation of $1.4 \mu\text{m}$ in Table 7 corresponds to a random surface error of $\pm 81 \text{ nm}$ ($\pm 2\sigma$ limits). This corresponds to the total surface error before the demagnification factor is applied. Given this and subtotal before demagnification in the table below, we can compute

that the $2.7 \mu\text{m}$ polishing allocation in the table corresponds to $\frac{2.7}{3.13} \times 81 = \pm 70 \text{ nm}$. For the

mean wavelength of the w bandpass, this is equivalent to a surface polish of $\lambda/8.7$. Likewise, the actuator errors correspond to a random surface error of $\pm 26 \text{ nm}$. And the wind loading errors correspond to $\pm 13 \text{ nm}$.

Figure 3 shows the secondary mirror structure function assuming a small scale surface roughness of $\sigma_{ss} = 14.3 \text{ nm}$, an $R_0 = 102.6 \text{ cm}$, and with tilt compensation. Table 8 is for the convenience of the polishing vendor. It shows the values of the points displayed as red boxes in Figure 3. The construction of the structure functions from values of σ_{ss} and R_0 was described in Section 4.2. For the secondary mirror we have used the diameter of the secondary mirror itself for D in the equations describing the M2 structure function.

Table 7. Secondary Mirror Image Budget

5-Mar-08

PS4 M2 Image Budget

Footprint = 782

	RMS Radius (um)		R0 (cm)		FWHM (arcsec)	
	z=0	z=70	z=0	z=70	z=0	z=70
Axial Support	0.4	1.4	692.65	197.90	0.01	0.05
Lateral Support	0.3	1.9	923.53	145.82	0.01	0.07
Actuator Errors	0.7	1.5	395.80	184.71	0.03	0.05
Wind Loading	0.5	1.0	554.12	277.06	0.02	0.04
Glass Inhomogeneity	0.1	0.1	2770.60	2770.60	0.00	0.00
Temp. Non-uniformities	0.1	0.1	2770.60	2770.60	0.00	0.00
Reflective Coating	0.5	0.5	554.12	554.12	0.02	0.02
Polishing	4.0	4.0	69.27	69.27	0.15	0.15
Subtotal	4.15	5.01	66.71	55.32	0.15	0.18
2.30 Demagnification	1.80	2.18	153.55	127.34	0.07	0.08
(Tele. Image Budget)	1.8	2.3	153.92	120.46	0.07	0.08

Table 8. Secondary Mirror Structure Function Specification

(This needs modification!)

Separation (cm)	RMS Surface Error (nm)
1.6	10.8
2.0	11.0
2.5	11.4
3.2	11.9
4.0	12.6
5.0	13.5
6.3	14.6
7.9	16.0
10.0	17.7
12.6	19.8
15.8	22.1
20.0	24.9
25.1	27.8
31.6	30.8
39.8	33.6
50.1	35.5
63.1	35.4
79.4	30.3

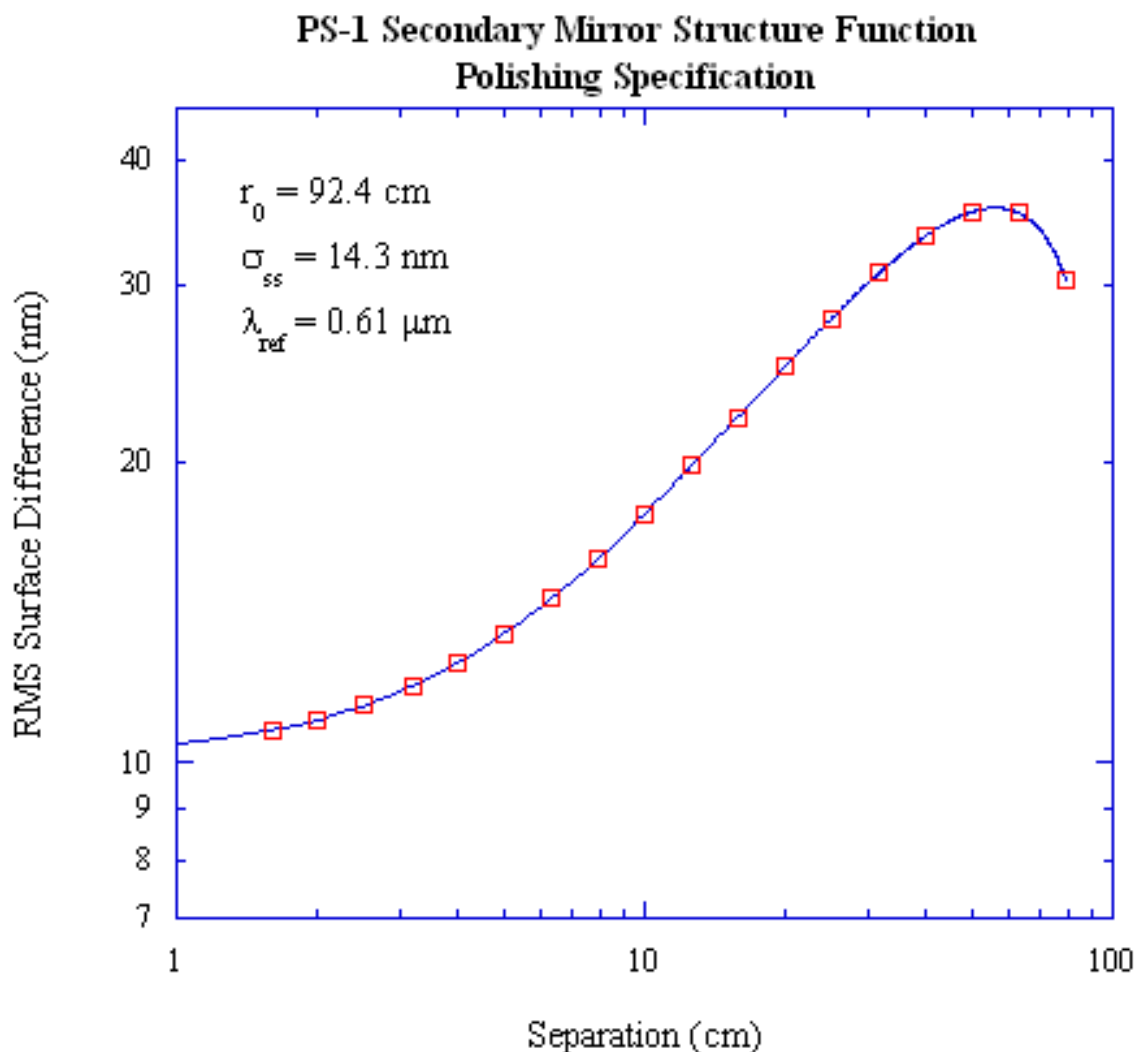


Figure 3. The PS4 Secondary Mirror Structure Function. The red boxes illustrate the data points given in Table 8.

4.4 L1 corrector error allocations

The L1 corrector is the closest corrector element to the secondary mirror. In the current baseline optical designs, this is a single element lens, but it is anticipated that this element will be replaced by an Atmospheric Dispersion Corrector (ADC). The current Pan-STARRS ADC design is susceptible to both hydrostatic and temperature effects in the siloxane that is used to inhibit ghosting and to increase throughput. As such, the support errors and the errors from temperature non-uniformities are given significant allocations.

The footprint for this optic is only 272 mm, and the subsequent magnification is high. This should be kept in mind for this and all subsequent tables in comparisons of errors in the different tables.

The decenter, tilt, and despace allocations for this optic (and for all of the correctors) were made based on a comparison of the magnitudes of the motions that these allocations imply with distances that are routinely obtainable with normal machine shop practices. Zemax tolerance calculations were used to determine that the alignment tolerances in Table 9 imply the following motion limits to the L1 optic:

- Decenter ≤ 0.2 mm (0.008")
- Tilt ≤ 0.6 arcminutes (0.05 mm at a radius of 300 mm = 0.002" at a radius of 11.81")
- Despace ≤ 0.3 mm (0.012")

Table 9. L1/ADC Corrector Image Budget

5-Mar-08

PS4 L1 Corrector Image Budget

Footprint = 272

	RMS Radius (um)		R0 (cm)		FWHM (arcsec)	
	z=0	z=70	z=0	z=70	z=0	z=70
Lens Support	3.0	5.8	92.35	47.77	0.11	0.21
Siloxane	2.0	3.8	138.53	72.91	0.07	0.14
Temp. Non-uniformities	3.0	3.0	92.35	92.35	0.11	0.11
Glass Inhomogeneity	0.5	0.5	554.12	554.12	0.02	0.02
Polishing	2.5	2.5	110.82	110.82	0.09	0.09
Subtotal	5.34	7.97	51.90	34.75	0.19	0.29
6.62 Demagnification	0.81	1.20	343.44	229.94	0.03	0.04
Decenter	1.25	2.00	221.65	138.53	0.05	0.07
Tilt	1.25	1.90	221.65	145.82	0.05	0.07
Despace	1.25	1.40	221.65	197.90	0.05	0.05
Subtotal	2.31	3.32	119.91	83.45	0.08	0.12
(Tele. Image Budget)	2.4	3.3	115.44	83.96	0.09	0.12

Zemax tolerance calculations using the TEZI macro indicate that the 2.3 μ m error allocation in Table 9 corresponds to a random surface error of ± 493 nm ($\pm 2\sigma$ limits). The 2.5 μ m polishing allocation therefore corresponds to a random surface error of

$$\frac{2.5}{5.34} \times 493 = \pm 231 \text{ nm, or a surface polish of } \lambda/2.6.$$

4.5 L2 corrector error allocations

Zemax tolerance calculations were used to determine that the alignment tolerances in Table 10 imply the following motion limits to the L2 optic:

- Decenter ≤ 0.15 mm (0.006")
- Tilt ≤ 1.0 arcminutes (0.09 mm at a radius of 300 mm = 0.003" at a radius of 11.81")
- Despace ≤ 0.2 mm (0.008")

Table 10. L2 Corrector Image Budget

5-Mar-08

PS4 L2 Corrector Image Budget

Footprint = 231.2

	RMS Radius (um)		R0 (cm)		FWHM (arcsec)	
	z=0	z=70	z=0	z=70	z=0	z=70
Lens support	4.0	8	69.27	34.63	0.15	0.29
Temp. Non-uniformities	2.0	2.0	138.53	138.53	0.07	0.07
Glass Inhomogeneity	0.5	0.5	554.12	554.12	0.02	0.02
Polishing	3	3	92.35	92.35	0.11	0.11
Subtotal	5.41	8.79	51.23	31.52	0.20	0.32
7.79 Demagnification	0.69	1.13	398.84	245.42	0.03	0.04
Decenter	1.8	2.30	153.92	120.46	0.07	0.08
Tilt	1.5	1.80	184.71	153.92	0.05	0.07
Despace	1.30	1.50	213.12	184.71	0.05	0.05
Subtotal	2.77	3.47	100.09	79.80	0.10	0.13
(Tele. Image Budget)	2.8	3.5	98.95	79.16	0.10	0.13

The Zemax TEZI tolerance calculations confirm that the allocation of 2.2 μm in Table 10 is equivalent to a random surface error of ± 781 nm. The polishing specification of 1.5 μm for this optic therefore corresponds to a surface error of $\frac{1.5}{3.94} \times 781 = \pm 297$ nm, which is only a

$\lambda/2$ polishing specification. The small polishing specification of 1.5 μm is the result of a rapidly converging beam and therefore a large demagnification factor and does not clearly reveal the fact that this optic has a looser polishing specification than previous surfaces.

4.6 L3 corrector error allocations

Zemax tolerance calculations were used to determine that the alignment tolerances in Table 11 imply the following motion limits to the L3 optic:

- Decenter ≤ 0.15 mm
- Tilt ≤ 3.6 arcminutes
- Despace ≤ 0.3 mm

Zemax tolerance calculations with the TEZI macro show that a total allocation of $0.28 \mu\text{m}$ corresponds to a random surface error of ± 247 nm. The polishing allocation of $8 \mu\text{m}$

corresponds to a random surface error of $\frac{8}{9.95} \times 247 = \pm 199$ nm, which is a $\lambda/3.1$ surface polish.

Table 11. L3 Corrector Image Budget

5-Mar-08

PS4 L3 Corrector Image Budget

Footprint = 50.6

	RMS Radius (μm)		R0 (cm)		FWHM (arcsec)	
	z=0	z=70	z=0	z=70	z=0	z=70
Lens Support	5.0	7.6	55.41	36.46	0.18	0.28
Temp. Non-uniformities	3.0	3.0	92.35	92.35	0.11	0.11
Glass Inhomogeneity	1.0	1.0	277.06	277.06	0.04	0.04
Polishing	8.0	8.0	34.63	34.63	0.29	0.29
Subtotal	9.95	11.48	27.85	24.14	0.36	0.42
35.57 Demagnification	0.28	0.32	990.55	858.63	0.01	0.01
Decenter	1.20	1.40	230.88	197.90	0.04	0.05
Tilt	1.20	1.40	230.88	197.90	0.04	0.05
Despace	0.80	0.90	346.33	307.84	0.03	0.03
Subtotal	1.90	2.20	146.06	126.01	0.07	0.08
(Tele. Image Budget)	1.9	2.2	145.82	125.94	0.07	0.08

4.7 Filter error allocations

The Pan-STARRS filters are flat without optical power and far from focus. The telescope PSF is unaffected by large changes in the filter position along the optical axis. Therefore there is no error budget for despace. Likewise, the PSF is unaffected by movements of the filters perpendicular to the optical axis. Therefore there is no error budget for decenter. There is a weak dependence of the PSF on the filter tilt. The tilt error allocation given in Table 12 corresponds to a tilt ≤ 50 arcminutes.

Zemax tolerance calculations with the TEZI macro show that a total allocation of $0.39 \mu\text{m}$ corresponds to a random surface error of $\pm 344 \text{ nm}$. The polishing allocation of $9 \mu\text{m}$

corresponds to a random surface error of $\frac{9}{9.75} \times 344 = \pm 318 \text{ nm}$, which is a $\lambda/1.9$ surface polish.

Table 12. Filter Image Budget

5-Mar-08	PS4 Filters Image Budget					
	Footprint = 72					
	RMS Radius (um)		R0 (cm)		FWHM (arcsec)	
	z=0	z=70	z=0	z=70	z=0	z=70
Lens Support	3.0	5.8	92.35	47.77	0.11	0.21
Temp. Non-uniformities	2.0	2.0	138.53	138.53	0.07	0.07
Glass Inhomogeneity	1.0	1.0	277.06	277.06	0.04	0.04
Polishing	9.0	9.0	30.78	30.78	0.33	0.33
Subtotal	9.75	10.94	28.43	25.33	0.36	0.40
25.00 Demagnification	0.39	0.44	710.64	633.25	0.01	0.02
Tilt	0.30	0.60	923.53	461.77	0.01	0.02
Subtotal	0.49	0.74	563.20	373.10	0.02	0.03
(Tele. Image Budget)	0.5	0.7	554.12	395.80	0.02	0.03